九州大学学術情報リポジトリ
Kyushu University Institutional Repository

A Study on Shear Loading Capacity of SRC Beams and Load Transfer Mechanism of Connection in Hybrid Frame Piers

Tomoda, Tomoo
Nippon Koei Co., Ltd., Tokyo Office : Project Leader

Yamaguchi, Kohei
Department of Civil and Structural Engineering : Research Associate

Guo, Shenghua
Department of Urban and Environmental Engineering : Graduate Student

Hino, Shinichi
Department of Civil and Structural Engineering : Professor

https://hdl.handle.net/2324/3287

出版情報：九州大学工学紀要. 65 (3), pp.115-128, 2005-09. 九州大学大学院工学研究院
バージョン：
権利関係：

KYUSHU UNIVERSITY

Memoirs of the Faculty of Engineering, Kyushu University, Vol.65, No.3, September 2005

A Study on Shear Loading Capacity of SRC Beams and Load Transfer Mechanism of Connection in Hybrid Frame Piers

by

Tomoo TOMODA[*], Kohei YAMAGUCHI[**], Shenghua GUO[***]

and Shinichi HINO[†]

(Received August 8, 2005)

Abstract

In recent years, the hybrid rigid frame bridge, which consist of a continuous girders and RC piers, has been widely used due to its low cost and its seismic safety. On the other hand, structures that have the spaces below their viaducts can be used in urban highways, the application of RC rigid frame piers is effective. However, no basic research has been performed and no design method has been established so far for a hybrid frame piers consisting of a few girders bridge and RC rigid frame piers. Therefore, we examined the shear loading capacity of SRC cross beam and the flexural loading capacity of the knee joint in the hybrid frame piers by the loading test and the FEM analysis.

The results show that the shearing force does not change even if the full web steel frame of various types is used to SRC cross beam, and clarified the load transfer mechanism and the stiffening structure of knee joint with a main I-girder.

Keywords: Shearing test, SRC Beams, Hybrid frame piers, FEM, Bending test, Knee joint

1. Introduction

In the highway bridge design, attention should be paid to the hybrid rigid frame bridge[1)] with integrated superstructure and substructure construction that has been widely used in consideration of the maintenance cost and seismic safety. Thus, researchers experimented on a knee joints with steel I-girders, and proposed new hybrid frame piers as shown in **Fig.1**. To enhance economical of

[*] Project Leader, Nippon Koei Co., Ltd., Tokyo Office
[**] Research Associate, Department of Civil and Structural Engineering
[***] Graduate Student, Department of Urban and Environmental Engineering
[†] Professor, Department of Civil and Structural Engineering

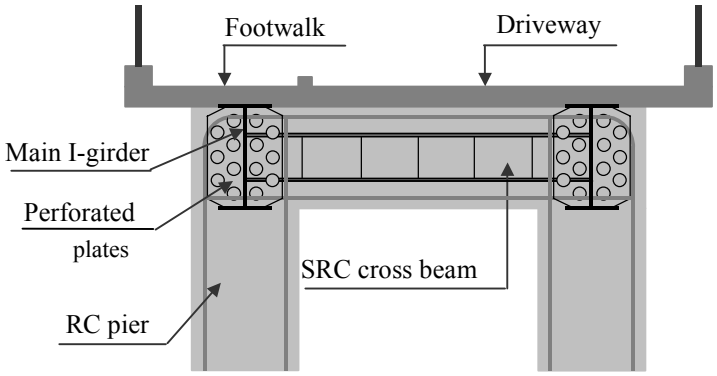

Fig.1 Proposed hybrid frame piers.

the cross beam, cost curtailment is possible by improving the SRC (steel reinforced concrete) beam which served as the cross-tie member for the main I-girders. And, simplification of knee joints with RC (reinforced concrete) pier and the improvement of workability at the time of concrete casting are expectable.

Moreover, as the cross beam span is too short to design RC rigid frame piers, the shearing strength as well as the flexural strength in case of a massive earthquake becomes a dominant factor. In the design of RC rigid frame piers[2], it is appropriate to provide a stirrup or adopting a beam height. However, in the hybrid frame piers, the shearing strength and the freedom of design are improved by adopting a SRC cross beam. Although the calculation formula of the shearing strength for a SRC beam is shown in Guidelines for performance-based design of steel-concrete hybrid structures of JSCE (thereafter, Guidelines) [3], it is not clear whether it is applicable to the SRC cross beam in which a shear span ratio is small or in which both ends are restrained by the main I-girders.

The purpose of this paper is to examine by load test and FEM analysis (a) the compatibility of the existing calculation, (b) the influence of the main I-girder web and the steel frame stiffener, (c) the effectiveness of the steel framed flange, because these factors are not clear in the existing calculation, and (d) the flexural loading capacity of the knee joint, which is united with the steel frame of the SRC cross beam.

2. Shear Loading Test of SRC Beams

2.1 Outline of specimen and shear loading test

The details and material properties of the specimens used are shown in **Fig. 2** and **Tables 1** and **2**. Specimens were produced for various beam types: RC beam (type-A) to be used as a comparison basis: SRC beam (type-B) which has a narrow flange width according to the existing calculation for shear loading capacity: general SRC beam (type-C): and the SRC beam (type-D) which has an intermediate stiffener and an end stiffener as a real bridge. Furthermore, in order to examine the influence restrained by the main I-girder web at both ends, specimens for type-B' and type-C' beams with the end stiffener attached to the steel frame were added. The concrete strength and reinforcement arrangement of each specimen are same as type-A specimen. The shear span ratio was determined from the cross sectional dimension similar to a real bridge and the dimension in which the bending failure of the specimen does not occur. Moreover, loading tests were carried out for twice by the six kinds of specimens.

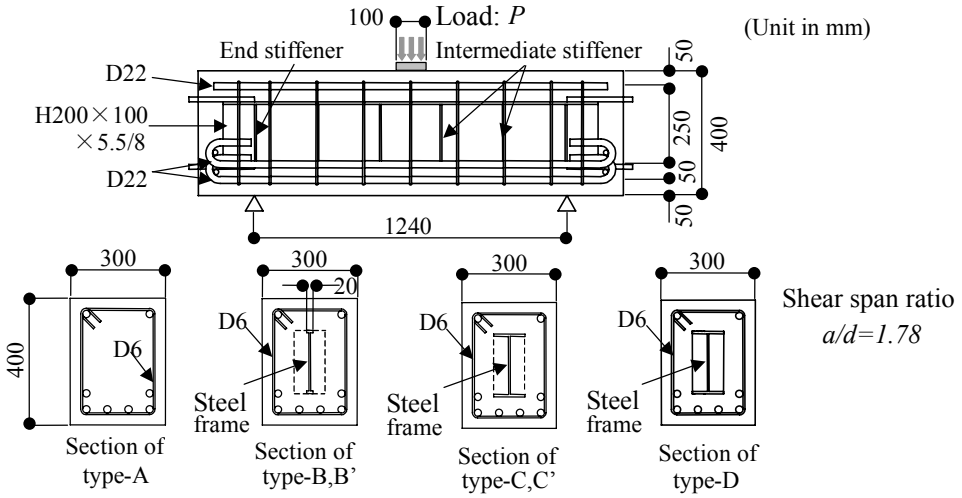

Fig. 2 Detail of specimens.

Table 1 Material property.

(a) Material properties of concrete

Specimen	Design strength(N/mm^2)	Compressive strength(N/mm^2)	Young's modulus(N/mm^2)	Tensile strength(N/mm^2)
1st test	30	26.1	2.4E+04	2.6
2nd test	30	30.4	2.8E+04	2.6

(b) Material properties of steel

Component	Grade	Dimension	Yield strength (N/mm^2)	Tensile strength (N/mm^2)
Reinforcement	SD345	D22	412	579
Stirrup	SD295	D6	383	530
Steel Form	SS400	H-200	381	483

Table 2 Type of specimens.

Specimen	Structure	Flange width(mm)	End stiffener	Intemediate stiffener
type-A	RC			
type-B	SRC	20	not add	not add
type-B'	SRC	20	add	not add
type-C	SRC	100	not add	not add
type-C'	SRC	100	add	not add
type-D	SRC	100	add	add

Concentric load, which adds a uniform load on the 100mm by 300mm width of the beam center section, was used for the loading approach. First, the test at the design allowable load of the RC beam; P_d=540kN was repeated twice, next the test at the design allowable load of the SRC cross beam; P_d'=800kN was repeated twice to the maximum shear load at the last test, and the loading step was increased. The strain of steel frame, reinforcement and concrete, deflection of the center of the beam span and the crack distribution of concrete were measured.

2.2 Ultimate Shear Load

The design shearing strength (V_{ud}) and test value (V_{ud}') of a specimen are shown in **Table 3**. The ultimate shear load was calculated by Eq. (1), which was based on Guidelines. However, the influence of a shear span ratio was taken into consideration only in the concrete part (V_{cd}), which is clear in RC beams[3].

$$V_{ud} = \alpha \cdot V_{cd} + V_{sd} + V_{rd} \quad (1)$$

Where V_{cd} : Design shear load of concrete
V_{sd} : Design shear load of stirrup
V_{rd} : Design shear load of steel frame web plate
α : Influence coefficient of shear span ratio (a/d).
$[\ \alpha = 3/(a/d),\ \ 0.5 \leqq a/d < 3.0]$

Table 3 shows that the addition of stiffener to the steel frame web plate has no apparent influence on the ultimate shear load. It also shows that the shearing strength increases, although slightly by adding a steel framed flange. Furthermore, Eq. (1) is applicable to the cross beam of hybrid frame piers enough, but it is considered to overestimate a little compared with the test value.

2.3 Crack distribution

The crack distributions of specimens are described in **Fig.3**. The photographs of the ultimate state observed at the 1st loading test show the specimen's type and ultimate load.

First, the type-A beam was loaded by P=83kN and the bending crack occurred at the center of the span, and then the shear crack occurred at load P=300kN. And, if the load is increased, the slanting crack extends, and brittleness failure was caused by ultimate load P_{max}=792kN. Next, the type-B beam was loaded by P=120kN and the bending crack occurred, and then the shear crack occurred at load P=300kN. The slanting crack extends with the increase of load, and shear failure was caused by ultimate load P_{max}=1045kN. Next, the type-C beam was loaded by P=100kN and

Table 3 Test results of shearing strength.

Specimen		Test value (kN)		Design value V_{ud} (kN)	Test value / Design value
		Max. load : P_{max}	Shearing strength: V_{ud}'		
type-A	1st	792	396	333	1.19
	2nd	797	399	358	1.11
type-B	1st	1045	523	555	0.94
	2nd	1043	522	581	0.90
type-B'	1st	1073	537	555	0.97
	2nd	945	473	581	0.81
type-C	1st	1129	565	555	1.02
	2nd	1124	562	581	0.97
type-C'	1st	1079	540	555	0.97
	2nd	1058	529	581	0.91
type-D	1st	1081	541	555	0.97
	2nd	1061	531	581	0.91

bending crack occurred, then shear crack occurred at the same load P=300kN as the type-B beam. Although shear failure was caused by ultimate load P_{max}=1129kN, the crack with a shape like a parabola, which connects the loading point and supports at the time of failure, was seen. Finally, the type-D beam was loaded by P=83kN and the crack occurred, and then crack of bending moment increased with the load. Moreover, when the load increased to P=300kN, the crack shifted to shear crack, and shear failure was caused by ultimate load P_{max}=1081kN.

From these, all specimens were judged to be shear failure from the crack propagation of concrete, and the strain of a tension-side reinforcement. And, a shear crack and shear failure have generated the SRC cross beam from type-B to D by the same load, and it is indicated that there is no difference of ultimate state. However, bending crack tends to distribute a little at type-D, which has an intermediate stiffener and an end stiffener.

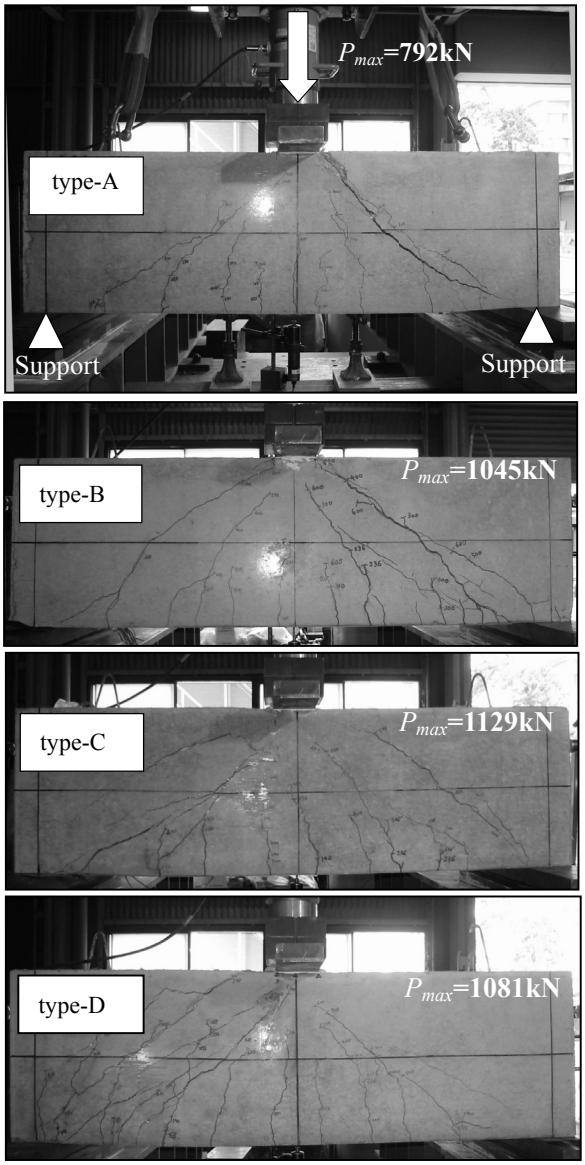

Fig.3 Crack distribution of max. load (1st test).

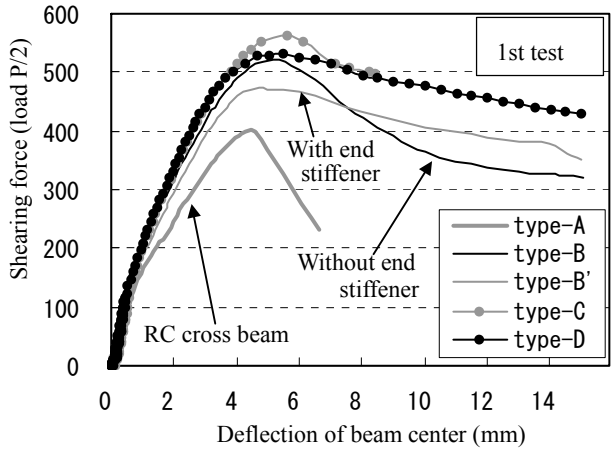

Fig.4 Load-deflection curve (type-A, B, B', C, D).

2.4 Post-peak behavior of SRC beam

The loads of type-A, B, B', C and D beams, and deflection at the span center are shown in **Fig.4**.

When RC beam of type-A reached the maximum load, the reduction of load and the increase of vertical deflection advanced rapidly, but as for type-B, C and D beams which have the SRC cross beam, the reduction of load and the increase of vertical deflection even after post-peak advanced slowly. Moreover, in order to consider the influence of a steel framed flange, the type-B beam was compared with type-C and D beams, and it was observed that the deformation behavior after post-peak of type-C and D beams that have a steel framed flange was the smallest. Furthermore, in order to consider the influence of the end stiffener, the type-B beam was compared to the type-B' that has no steel framed flange and the result was that the deformation behavior after post-peak of the type-B' beam, which had an end stiffener added to the steel frame web plate, was smaller.

The results showed that RC beams are subject to brittleness shear failure under the above conditions, but their toughness can be increased by transforming them into SRC cross beam. Moreover, if an end stiffener and an intermediate stiffener are added to the steel frame web plate, it will increase the toughness of SRC cross beams after post-peak. The same effectiveness is also achieved in the case of applying a flange to the steel frame.

3. Simulation by FEM Model

3.1 FEM model

In order to examine the stress distribution of beam specimen, 3-dimension nonlinear analysis was conducted using LUSAS[4]. The analysis model as shown in **Fig.5** was considered to be partial model using the symmetry of a specimen of 4 divisions. The finite element and an ingredient model as shown in **Table 4** and **Fig.6** uses 8-node solid components for concrete, 4-node shells for steel frame and 2-node bar components for reinforcement. For concrete material, the linear elastic model was used before crack, and the strain-softening model was used after crack generation.

3.2 Comparison of shear loading test and FEM analysis

The shearing capacity at the 2nd loading test, the FEM analysis results and the results of

calculation by Eq. (1) are shown in **Table 5**. Therefore a comparison of the shear loading capacity in the cases with and without a stirrup by the FEM analysis is shown in **Table 6**.

According to the test values, the shearing capacity of type-A, B and C beams becomes higher than the FEM analysis results, but that of the type-D beam with an intermediate stiffener is 9% lower. Moreover, in the FEM analysis, the shearing capacity of type-C, C', and D beams with the steel framed flange is higher than that of type-B and B' beams. Furthermore, in the FEM analysis of the cases with and without a stirrup type-C and D beams having stirrup appear more effective than the type-B beam, which does not have the steel framed flange. Even compared with the design values of the stirrup (V_{sd}), the increase of a shearing strength is larger than type-B.

From these results, it can be judged that the shearing strength of the SRC cross beam increases owing to the steel framed flange. It is indicated that the steel framed flange and the stirrup have an interaction that improves the shear capacity of the SRC cross beam by restraining internal concrete.

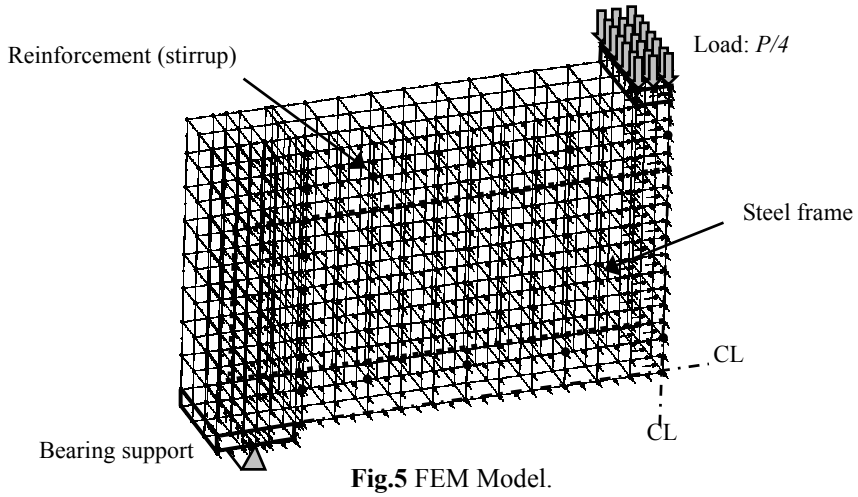

Fig.5 FEM Model.

Table 4 Analysis conditions.

Application program		LUSAS ver. 13.5
Elements	Concrete	3D Solid continuum elements
	Reinforcement	Bar elements
	Steel frame	Thick shell elements
Hardening rule	Reinforcement Steel frame	Yield criterion of von Mises

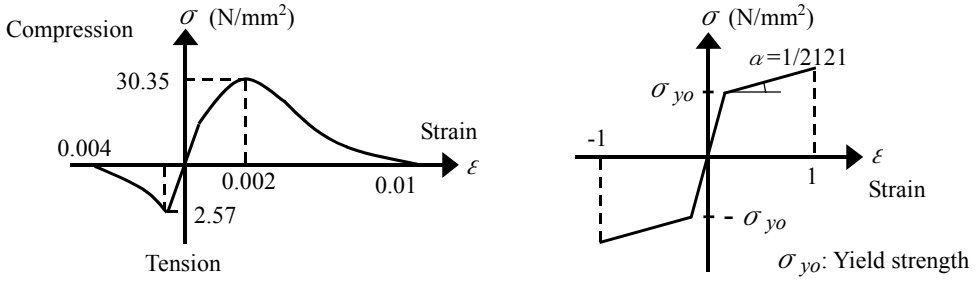

(a) Material model of concrete (b) Material model of steel

Fig.6 Material model.

Table 5 Test, FEM and design value of shear loading capacity.

Specimen	Shear loading capacity of 2nd test (kN)			Test value / FEM value	Design value / FEM value
	Test value	FEM value	Design value		
type-A	399	360	358	1.11	0.99
type-B	522	488	581	1.07	1.19
type-B'	473	467	581	1.01	1.24
type-C	562	546	581	1.03	1.06
type-C'	529	586	581	0.90	0.99
type-D	531	584	581	0.91	0.99

Table 6 Comparison of shear loading capacity by FEM.

Specimen	Stirrup	FEM value; (1)	add−not add; (2)	V_{sd} ; (3) Design value	(2)-(3)
type-A	add	360	56	Design shear load of stirrup , 35kN	21
	not add	304			
type-B	add	488	39		4
	not add	449			
type-C	add	546	64		29
	not add	482			
type-D	add	584	87		52
	not add	497			

4. Bending Test of Hybrid Frame Piers

4.1 Outline of specimen and bending test

When an earthquake motion generated at the direction perpendicular to bridge axis on a hybrid frame pier, the bending moment will transmit to the core of the knee joint through the main I-girder which is united with the steel frame of SRC cross beam. Then, it is important to design the knee joint of SRC cross beam and RC pier, bending test was performed on specimen and the load-carrying capacity of the knee joint was examined[5].

A specimen is an L form model, which imitated the knee joint of the hybrid frame pier, and is reproducing the case with inadequate reinforcing bar of the knee joint by the main I-girder of superstructure, and a new stiffening structure. The detail and material properties of the specimen are shown in **Figs.7, 8** and **Table 7**. A cross beam is SRC structure which used the full web beam, and the pier consists of RC cross sections. The main I-girder of the superstructure which penetrates the knee joint was reproduced by embedding steel I-girder, one type manufactured what does not have reinforcing bar in the knee joint (hereafter, without perforated plates), and one other type manufactured what added two perforated plates[6] to the steel I-girder's web on each side (hereafter, with perforated plates). Moreover, the perforated plate is designed so that the tensile strength[7] generated to the concrete of the knee joint can be resisted.

We deal here with that the bending moment of the direction closed to the L type specimen acts. The loading approach became it tense about the PC bar with the hydraulic jack so that the end of the pier and SRC cross beam might be closed. Although a loading step is shown in **Fig.9**, the load is increased to the small-scale seismic load (level 1) by the specifications for Japanese highway bridges[7] (hereafter, SPEC), and the tensile reinforcement of the pier becomes allowable strength

(σ_{ta} =140N/mm^2), and up to the large-scale seismic load (level 2) by SPEC, and then gradual increase loading was carried out to failure after that.

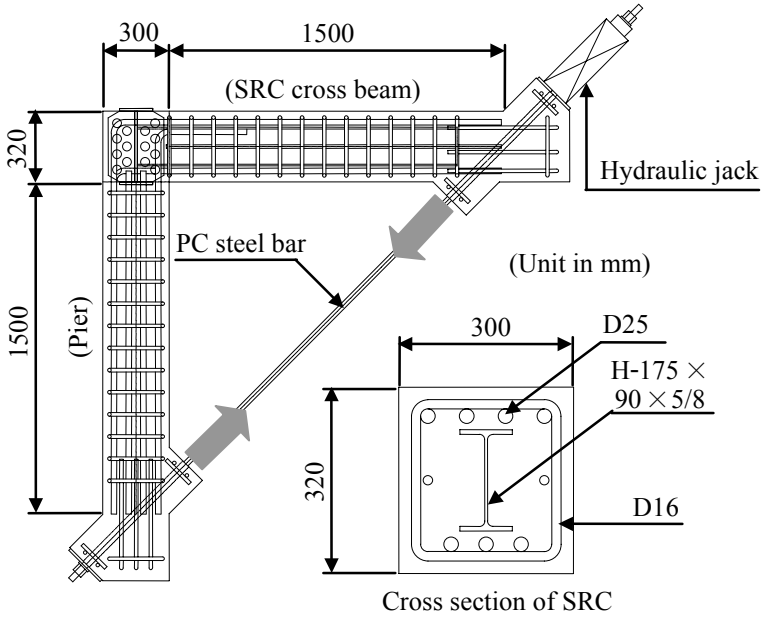

Fig.7 L-shaped specimen.

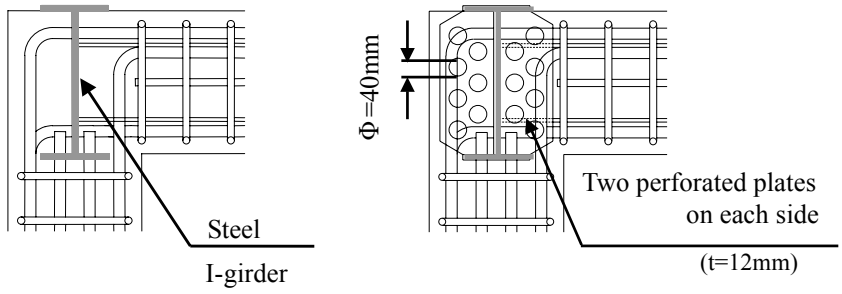

(a) Without perforated PL (b) With perforated PL

Fig.8 Detail of knee joint.

Table 7 Material properties.

(a) Material properties of concrete

Design compressive strength (N/mm^2)	Compressive strength (N/mm^2)	Young's modulus (N/mm^2)	Tensile strength (N/mm^2)
30	34.8	2.98E+04	3.40

(b) Material properties of steel

Component	Grade	Dimension	Yield strength(N/mm^2)	Tensile strength (N/mm^2)
Main I-girder	SS400	—	359	443
Perforated plates	SS400	—	312	441
Reinforcement	SD345	D25	406	641

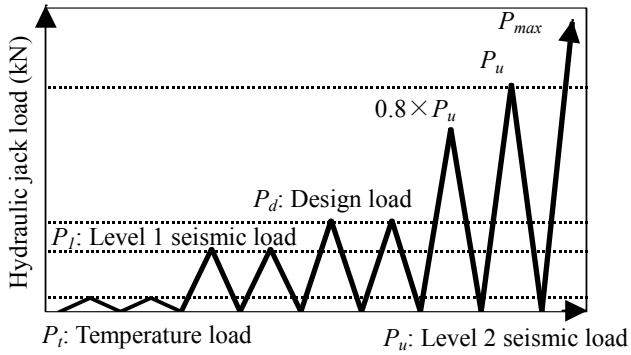

Fig.9 Loading step.

4.2 Results and discussion

(1) Deformation response

The relation between load and displacement of the load direction is shown in **Fig.10**, and the load value of bending test and design are shown in **Table 8**. The design value of the knee joint without perforated plates is a value, which calculated the cleavage load of concrete by SPEC[7),8)], and the design value with those plates is a value, which accelerated the cleavage resistance by perforated plates to it. Moreover, the deflection of the specimen without perforated plates is shown in **Fig.11**, and the deflection of the specimen with perforated plates is shown in **Fig.12**.

In the specimen without perforated plates, the cleavage crack of the knee joint occurred in the load of 52kN, which are the load-carrying capacity on a design, and it is expected that it would be in an ultimate state. However, the hybrid frame pier's knee joint brought a result, which has the load-carrying capacity far exceeding the design value to the bending moment of the closed direction. The cleavage crack occurred in the knee joint from near load 50kN, the pier reinforcement yielded at 167kN, and the reinforcement of SRC cross beam yielded at 172kN. Then, when the relative deflection of the loading's direction increased rapidly and the concrete of the pier base carried out compressive failure at 181kN, the knee joint broke at the same time and changed into the ultimate state.

On the other hand, the specimen with the perforated plates has large rigidity compared with other type, and deflection differs also from the ultimate state. The crack of the pier occurred at 12kN, and the reinforcement of the pier yielded at 199kN. Then, the reinforcement of SRC cross beam yielded at 203kN, and the concrete of the pier base carried out compressive failure at 222kN.

As for both specimens, although the test value of crack load (P_{cr}) is smaller than design value that is calculated by SPEC, the measured yield load of the reinforcement and the ultimate load correspond well with design value.

(2) Crack distribution of the knee joint

A crack distribution without perforated plates is shown in **Fig.13**, and that with perforated plates is shown in **Fig.14**. By the specimen with the perforated plates, the crack distribution differs from having no perforated plates greatly like deformation response.

In the specimen without perforated plates, the cleavage crack occurred in the diagonal direction of the knee joint at 50kN, but the knee joint has not lost the quality as a rigid frame. After that, the steel I-girder is changing into torsional deformation, and the clearance has produced it to the flange plate and concrete. There was no part, which the crack concentrated about the pier, or SRC cross beam, and the cleavage crack concentrated on the knee joint and broke to it changed into

the ultimate state. From these, it is indicated that knee joint's concrete suited the restricted state by the up and down flange of the steel I-girder which penetrates the knee joint.

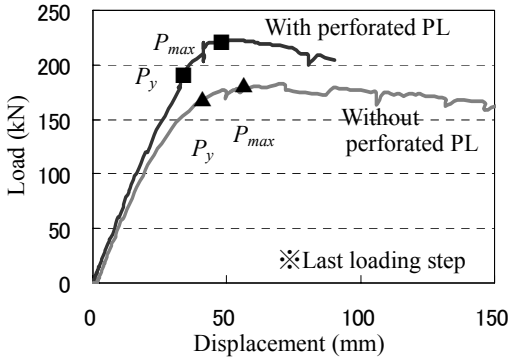

Fig.10 Load-displacement curve.

Table 8 Results of test and design value.

(Unit in kN)

			Cracking load : P_{cr}	Allowable load of reinforcement: P_d	Yield load of reinforcement: P_y	Ultimate load : P_{max}
RC pier	Design		21.6	64.6	187	187
	Test	with PL	12(0.56)	69(1.06)	199(1.06)	222(1.19)
		with no PL	14(0.63)	68(1.05)	167(0.89)	181(0.97)
SRC cross beam	Design		24	66.7	194	220
	Test	with PL	15(0.64)	70(1.05)	203(1.05)	—
		with no PL	16(0.65)	59(0.88)	172(0.88)	—
Knee joint	with PL	Design	—	—	—	233
		Test	—	—	—	222 or more
	with no PL	Design	—	—	—	52
		Test	—	—	—	181(3.51)

( ) shows the ratio to design value.

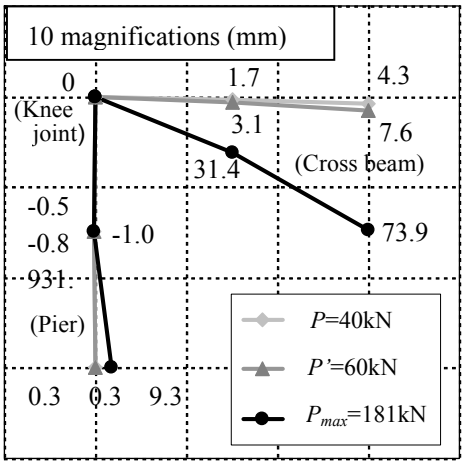

Fig.11 Deflection (without perforated PL).

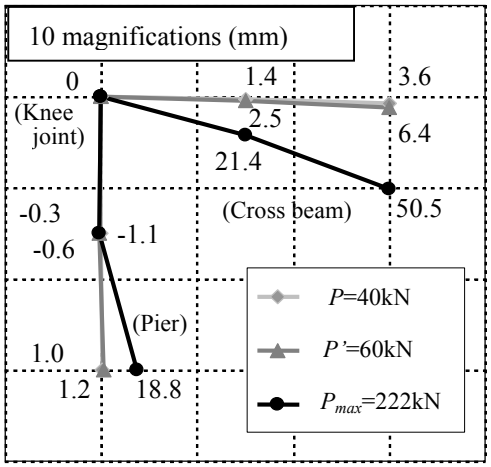

Fig.12 Deflection (with perforated PL).

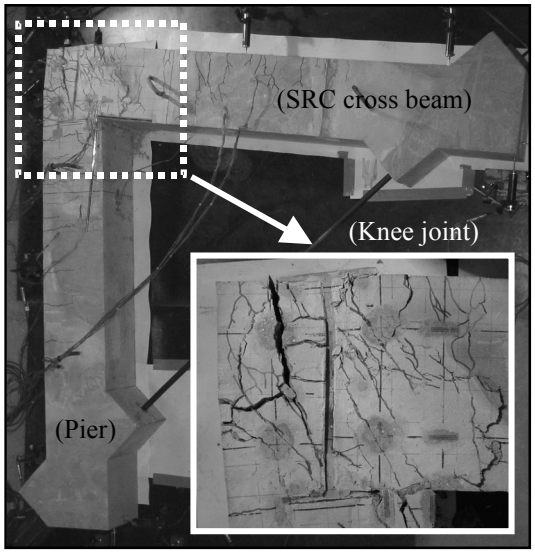

Fig.13 Crack pattern (without perforated PL).

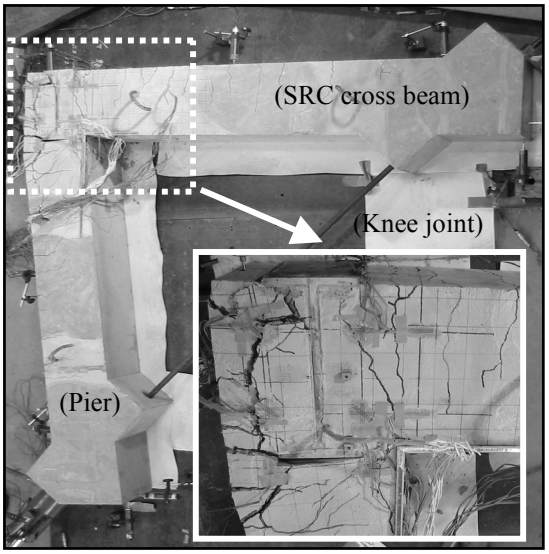

Fig.14 Crack pattern (with perforated PL).

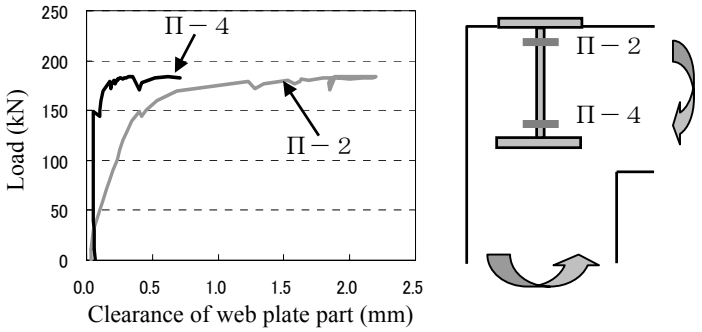

Fig.15 Load-clearance of web PL part (without perforated PL).

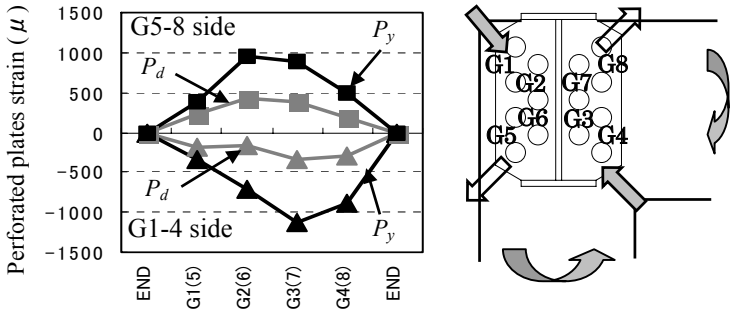

Fig.16 Strain distribution of perforated plates (with perforated PL).

On the other hand, the crack is concentrating the specimen with perforated plates on the pier upper side in which a plastic hinge is formed in case of a massive earthquake. Although the design ultimate strength of the knee joint was load 233kN and it was more than the ultimate load of the specimen, the covering of the knee joint cracked at the time of failure of the pier. However, when the core of the knee joint was checked at the time of demolition, it had not occurred a crack into the core part that reinforced with the perforated plates.

(3) Stress transfer state of the knee joint

When the excessive bending moment acts on the knee joint, the cleavage crack will occur to concrete with the tensile stress of the knee joint. Since the stress inside concrete cannot carry out direct measurement, it clarify the transfer state of the section force from the clearance between the steel I-girder, which penetrates the knee joint, and strain distribution of perforated plates.

In the specimen without perforated plates, after the cleavage crack occurred in the knee joint, the clearance was measured between the steel I-girder's web and concrete. The relation of the load and clearance of web plate part is shown in **Fig.15**. It was measured that the clearance of web top's part is increasing little after the load 50kN by which the crack was checked in the knee joint. The knee joint collapsed with torsional deformation of the steel I-girder on the ultimate load, then the concrete separated into both sides rapidly and has lost the function as the knee joint. From these results, deformation of concrete is restrained with the steel I-girder, and it is indicated that the ultimate strength of the knee joint improved by that I-girder.

In the specimen with perforated plates, the strain distribution of those plates was measured, which is shown in **Fig.16**. The strain of a diagonal direction became large in proportion to the increase of the bending moment. From this figure, it is indicated that the tensile member and the compressive strut are formed in the knee joint through the perforated plates.

4.3 Load transfer mechanism of the knee joint

The load transfer mechanism of the knee joint, which became clear from the bending test in the direction perpendicular to bridge axis, is shown in **Fig.17**.

When the bending moment exceeding the tensile stress of concrete acts, the load transfer mechanism will be formed in the knee joint. Compressive force of concrete (C_c, C_b) and tensile forces of reinforcement (T_c, T_b) act on the knee joint, and so the compressive strut of concrete and the tensile member are formed in the diagonal direction of that core part[9]. As the results, the section force between the pier and SRC cross beam is transmitted. Since the tensile force will make cleavage crack simultaneously, it is necessary to arrange the stiffening reinforcement, which resists tensile force in the knee joint. Therefore, perforated plates, which are the substitute stiffening reinforcement, are effective to the load transfer mechanism of the knee joint in hybrid frame piers.

On the other hand, the bending test without perforated plates proved that torsional resistance of steel I-girder transmits the bending moment of the knee joints, as shown in **Fig.18**.

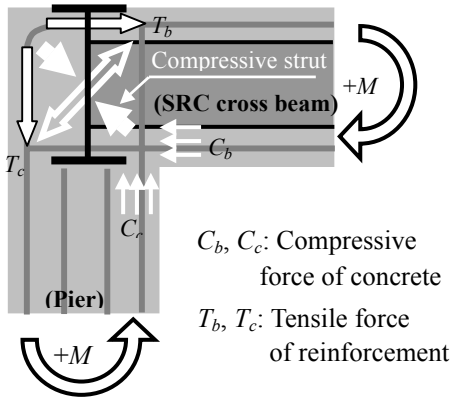

Fig.17 Load transfer mechanism.

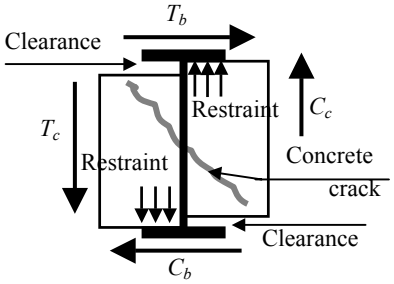

Fig.18 Restricted action by main I-girder (without perforated PL).

5. Conclusion

The following conclusions were clarified in this study.

(1) In the SRC cross beam of hybrid frame piers, when the design shearing strength was computed by existing calculation, it turned out that a little overestimation is given compared with the test value.

(2) The steel framed flange of SRC cross beams makes a little increase of shearing strength, and it controls the load loss after the maximum shearing strength and deformation.

(3) From the FEM analysis, it is proved that steel framed flange and stirrup raise effectively the shearing strength of the SRC cross beam.

(4) The knee joint of hybrid frame pier has very high load carrying capacity more than the ultimate load calculated by SPEC. It is based on torsional resistance of the steel I-girder which penetrates the knee joint.

(5) By adding perforated plates to the knee joint as an alternative member of reinforcing bar, the load transfer mechanism through that plate is formed in the knee joint. And it can transmit the bending moment of the SRC cross beam to the RC pier certainly.

(6) It turned out that the hybrid frame piers, which have the SRC cross beam and the connection of main I-girder, could be designed rationally and economically.

References

1) Expressway Technology Center: The technical report about hybrid structure of steel and concrete, 1997.

2) Japan Highway Public Corporation: Design guidelines the second collection, a bridge, a retaining wall and a culvert, 2003.

3) Japan Society of Civil Engineers: Guidelines for performance-based design of steel-concrete hybrid structures, pp.197- 206, 2002.

4) LUSAS Ver.13.5 User guide-element library, Finite Element Analysis Ltd, 2004.

5) Tomoo Tomoda, Shinichi Hino, Kohei Yamaguchi, Tomohiko Maekawa: An experimental study on the load transfer mechanism of the corner in RC rigid frame piers connected with main steel I girder, Proceedings of 59th JSCE annual conference, pp.1395- 1396, 2004.

6) June Nagata, Katsuyoshi Akihasi, Masayuki Watanabe: The perfobond plates pull-out test in consideration of the placing direction of concrete, Proceedings of 54th JSCE annual conference, pp.298- 299, 1999.

7) Japan Road Association: A specifications for highway bridges, I-IV, 2002.

8) Hiroshi Watanabe, Hirotaka Kono: Study on design method of RC knee joint, Civil Engineering Journal, 40-10, pp.36- 41, 1998.

9) M.J.N.Priestley, F.Seible, G.M.Calvi (Kazuhiko Kawashima editorial supervision): Seismic design and retrofit of bridges, Gihodo Shuppan, 1998.